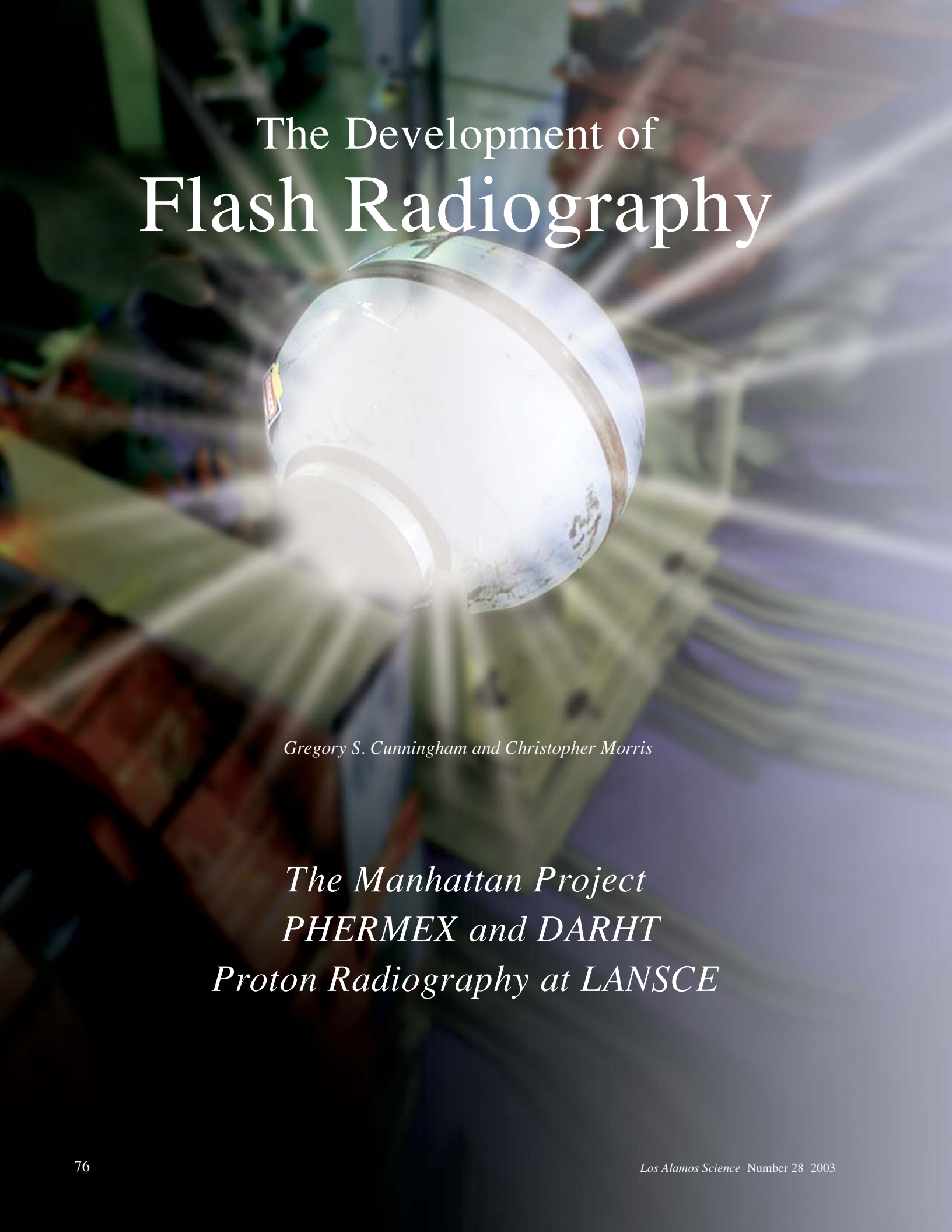

The Development of Flash Radiography

Gregory S. Cunningham and Christopher Morris

The Manhattan Project
PHERMEX and DARHT
Proton Radiography at LANSCE

In many ways, flash radiography is to nuclear weapons what medical x-radiography is to the human body: It allows one to see inside a complex structure without disturbing it. Starting in the Manhattan Project and continuing to this day, flash radiography has been used to take stop-action pictures of dynamic events: from the detonation of high explosives to the implosion of a mock weapon assembly containing a surrogate material for the nuclear core.

In this article, we will explain the basic principles of flash radiography and trace decades of progress in improving image quality. A major goal is to follow the hydrodynamic implosion, or hydrotest, to the point at which the surrogate core is maximally compressed. Los Alamos state-of-the-art x-ray hydrotests at the Dual-Axis Radiographic Hydrodynamic Test (DARHT) facility and facilities envisioned for the future will produce time-sequenced images of the implosion dynamics and provide views of the implosion along multiple lines of sight. Images from hydrotests at DARHT are already playing a crucial role in solving stockpile issues, including those related to the certification of remanufactured parts. A recent Los Alamos invention, proton radiography, is now fielded at the Los Alamos Neutron Science Center (LANSCE), the Laboratory's medium-energy accelerator facility. Proton radiography is also providing important data for the nuclear weapons program. A higher-energy proton radiography machine has the potential for providing a new level of quantitative precision and quality to the data from hydrotests.

Historical Origins

Quite remarkably, the best analog to our current experimental program in science-based stockpile stewardship is found in the program to develop the plutonium implosion bomb during the Manhattan Project. It was known from the start that enough fissionable material for a single bomb, either uranium-235 or plutonium-239, would not become available until late in the project. Consequently, the gun device—which propels one subcritical piece of fissionable material into another at high speed—was the favored method for assembling a supercritical mass. Because it was straightforward, this approach had the highest probability of success, whereas the spherical implosion of a subcritical configuration would present major technical challenges.

At that time, the nuclear properties of plutonium-239, the new manmade isotope, had been only crudely determined. When a barely visible speck of plutonium produced at Ernest O. Lawrence's cyclotron at the Berkeley Radiation Laboratory arrived at Los Alamos, scientists from the Physics Division used the material to measure more definitively the neutron number per fission and the cross sections for fission neutron capture and scattering. These were the first nuclear experiments completed at Los Alamos, and the results were encouraging. Because the neutron number for plutonium was indeed higher than that for uranium-235, plutonium would likely yield a more efficient nuclear explosion.

These measurements were fed into computational bomb design models as soon as they became available. Later, however, when reactor-produced plutonium arrived, the scientists detected a high neutron background, which, Enrico Fermi quickly showed, derived from the spontaneous fission of the isotope plutonium-240, a reactor byproduct present in the sample. Gun assembly of plutonium pieces containing plutonium-240 would be too slow to prevent premature initiation of the chain reaction by the neutrons from spontaneous fission, and therefore the likely outcome would be a fizzle rather than an efficient nuclear explosion. This finding forced the project to switch goals and aim for an implosion device.

In the implosion device, high explosives surrounding a spherical assembly would be detonated at many points, and the resulting converging spherical detonation wave would compress the nuclear material to a supercritical configuration. One had to measure the velocity of the implosion and the state of the metal during assembly in order to determine the optimal timing of the neutron initiators needed to achieve successful device performance. Director J. Robert Oppenheimer called this endeavor "one of the most urgent of the project's outstanding problems." Its solution occupied a talented group of physicists, chemists, and electrical and mechanical engineers. Details of the dynamic response of materials subjected to high-explosive drive were studied in small-scale experiments in GMX Division (predecessor of the present Dynamic Experimentation Division). To test the overall performance of the implosion device, the implosion group performed so-called "integral" experiments on mock assemblies, which had the correct geometry and components except for a nonfissionable, surrogate core in place of the plutonium pit.

As we discuss below, radiography with x-rays was a key diagnostic for those small-scale and integral tests and has remained so through the decades. In fact, many of the experimental tools developed in the 1940s to study the evolution of high-explosive-driven systems—electrically charged metal pins, optical framing cameras, and flash radiography—are still the standard diagnostics for monitoring weapons implosion. Today, through the use of vastly improved equipment and modern data acquisition and analysis methods, these tools are still helping us quantify important phenomena (such as the details of material failure and high-explosive detonation) and develop accurate, predictive physical

models to describe them. Before we trace the history of flash radiography for studying weapon implosion, we explain the basic principles of this technique, as well as some limitations that we hope to circumvent with advanced techniques.

Attenuation Radiography for Stockpile Stewardship

In modern hydrotests, we replace the fissionable pit of a nuclear primary with a mock pit made of a surrogate material such as natural uranium, lead, or tantalum. This nonnuclear system is imploded and its dynamics studied to provide constraints for the physics models used in numerical simulations of weapons performance. The primary diagnostic of hydrotest experiments is point-projection flash radiography. At the times of most interest, the experiment is illuminated with a short pulse of x-rays, and the transmitted flux (number of x-ray photons per unit area) is recorded on a suitably shielded detector.

Figure 1 is a diagram showing the geometry of a static experiment on the French test object (FTO), which was designed to allow French and U.S. experimenters to collaborate on flash radiography methods and analysis. High-energy x-rays are produced through the bremsstrahlung interaction of energetic—10 to 30 million electron volts (MeV)—electron beams with high-Z targets (that is, targets made of materials with high atomic numbers). Interaction with a positively charged nucleus causes an electron to bend (accelerate) and therefore radiate, or emit, photons. The loss of energy brakes its speed, hence the term bremsstrahlung (or braking radiation in German) for both the process and the emitted radiation. Although the emitted photons have a continuous energy spectrum, most of the photons that are transmitted through a

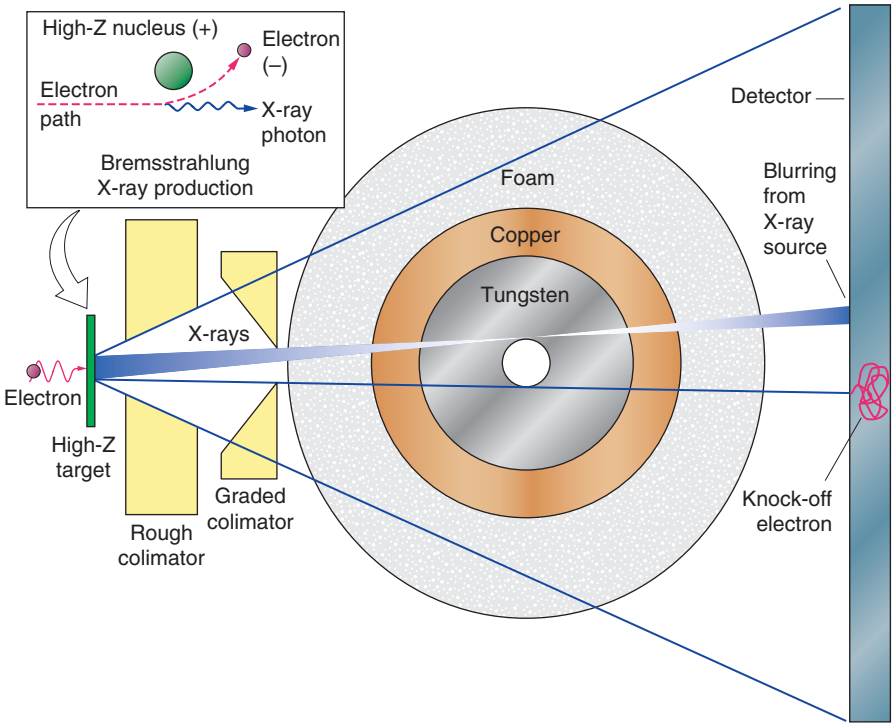

Figure 1. Basics of Flash X-Radiography

This schematic shows (from left to right) the production of x-ray pulses, their transmission through the so-called French test object (FTO), and their detection. At left, high-energy electrons (red) hit a high-Z target and interact with the heavy nuclei to produce x-rays (blue). The x-rays are attenuated by a rough collimator, which defines the field of view and then by a graded collimator that flattens the transmission profile to reduce scattering into the center of the image. The FTO consists of an inner spherical shell of tungsten (inner radius = 1 cm and outer radius = 4.5 cm) and an outer shell of copper (outer radius = 6.5 cm) surrounded by a shell of foam (outer radius = 22.5 cm). The location of material interfaces recorded at the detector are blurred because the x-ray source has a finite extent and because electrons knocked into motion by arriving x-rays have a finite range in the detector.

hydrotest assembly have an energy near 4 MeV. That energy is near the minimum in the absorption cross section for the materials in the assembly.

A crucial performance parameter that we would like to be able to measure with flash radiography is the density of the surrogate material at nuclear time—the time a "real" system would start producing a significant amount of nuclear energy. As we will discuss below, by measuring the attenuation of the x-ray flux transmitted through the center of the assembly, we can determine the integrated quantity ρ_A, the areal density, or line-of-sight mass, of the implosion system:

$$\rho_A = \int_0^L \rho(x,y,z)dz \ , \qquad (1)$$

where $\rho(x, y, z)$ is the volume density of the hydrotest object and z is the longitudinal coordinate through the assembly. For an object with constant density, ρ_0, the areal density is $\rho_0 \times L$, where L is the longitudinal thickness of the object.

Because the areal density of the system at nuclear times is very large, we need an enormous dose (that is, intensity × time) of x-rays to make the transmission measurement. The doses currently available, even from the lat-

est flash x-ray machines, are insufficient to provide the quality of data that weapons scientists will require to adequately constrain their calculations for future certification. In pursuit of better data quality, flash x-ray machines are being constantly upgraded and improved; at the same time, new data analysis technologies are being developed and implemented at Los Alamos and other weapons laboratories.

The most basic physics of transmission radiography is contained in the Beer-Lambert law, the solution to the differential equation that describes the number of particles surviving transport through a medium without interaction. The Beer-Lambert law can be derived from investigating transmission through an infinitesimally thin piece of material with constant density ρ_0 and thickness l. In this case, the probability that a particle goes through with no interaction is $(1 - \sigma\rho_0 l/A)$, where σ is the cross section for interaction in centimeters squared and A is the atomic mass in grams. For a material with finite thickness L, the probability of no interaction is

$$\lim_{n\to\infty}\left(1-\frac{\rho_0 L}{\lambda n}\right)^n = e^{-\frac{\rho_0 L}{\lambda}} \quad , \tag{2}$$

where $\lambda = A/\sigma$ is called the interaction length in grams per centimeter squared (gm/cm^2). Thus, if N_0 photons impinge on the material, then, on average, the number N that will make it through without interaction is given by

$$N = N_0 e^{-\frac{\rho_0 L}{\lambda}} \quad . \tag{3}$$

This equation can be generalized to materials with varying density as

$$N = N_0 e^{-\frac{\rho_A}{\lambda}} \quad , \tag{4}$$

where ρ_A is the areal density defined in Equation (1).

Equation (4) tells us that we can determine the areal density of the object in units of the interaction length λ of the incident radiation by measuring the ratio of incident to surviving particles:

$$\frac{\rho_A}{\lambda} = -\ln\left(\frac{N}{N_0}\right) \quad . \tag{5}$$

This simple analysis leaves out important details. For example, λ depends on energy, and the x-ray source is not monoenergetic. Also, scattered x-rays produce background "fog" in the image. Nevertheless, this simple analysis provides an important guide for evaluating and developing radiographic tools.

For example, we can calculate the uncertainty in the measured value of areal density, $\Delta\rho_A$, under the assumption that the only source of noise is the Poisson (counting) statistics of the transmitted beam. That uncertainty is given by

$$\frac{\Delta\rho_A}{\lambda} = \frac{1}{\sqrt{N}} \quad . \tag{6}$$

The optimal interaction length λ_{optimal} would be one that minimizes $\Delta\rho_A$ for a given object. Setting to zero the derivative of the uncertainty with respect to λ and solving for λ, we find that $\lambda_{\text{optimal}} = \rho_A/2$, or the optimum equals half the thickness (or areal density) of the object. For the FTO, ρ_A = 182.5 gm/cm^2, so the optimum interaction length is 91.75 gm/cm^2. Can we achieve such a long interaction length?

In the case of x-rays, λ varies strongly with x-ray energy. The interaction length reaches a maximum value at the energy at which the cross section for producing electron-positron pairs (that cross section increases with increasing energy) becomes comparable to Compton scattering (which decreases with increasing energy). The maximum interaction length of x-rays is weakly dependent on atomic number, Z, and therefore for all high-Z materials, λ is maximum at about the same x-ray energy, namely, near 4 MeV. The interaction length λ in uranium for 4-MeV x-rays is about 22 gm/cm^2, or a little over a centimeter in natural uranium, much smaller than the thickness of a hydrotest assembly. The relatively short interaction length of x-rays in heavy elements implies a large uncertainty in the areal density measurements, even when extremely high doses are used.

The First Radiographs of Implosion

Let us now go back to the origin of weapons radiography. In the spring of 1944, the Manhattan Project shifted its main focus to implosion after the discovery that reactor-produced plutonium had a high neutron background that was due to the presence of plutonium-240. The previous fall, John von Neumann had suggested that, with enough high explosive driving an implosion of a fissionable metal core, one could ignore the strength of the material and assume that the solid material behaved like a fluid. In this case, partial differential equations could be written and solved in a numerical program on IBM machines to determine the velocity of implosion. However, the input to the equations, that is, the high-explosive drive and the equation of state (EOS) of the metal and explosives needed to be determined. Flash radiography was one of the important diagnostic techniques used in quantifying the spherically converging high-explosive drive.

In the initial experiments conducted in 1943, Seth Neddermeyer's group tried surrounding a small metal sphere with weak explosive charges and detonating it at many points. The scientists expected the diverging spherical

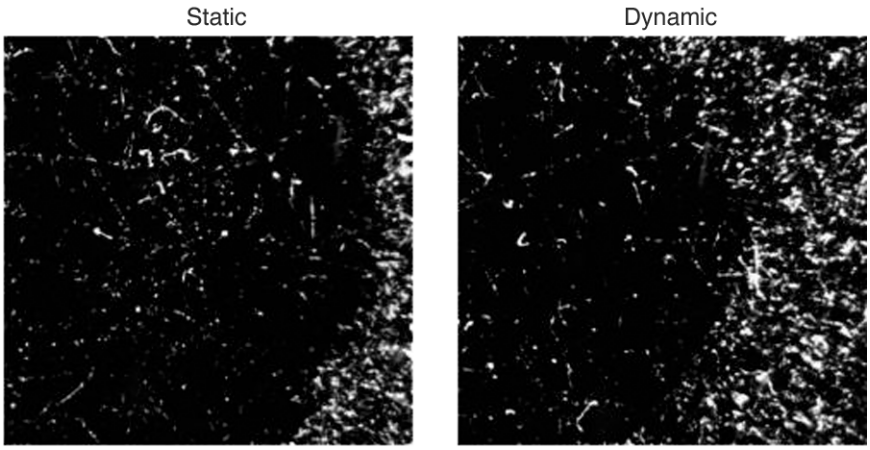

Figure 2. Radiographs of an Explosively Driven Implosion Experiment
These radiographs were taken in 1944 to image the outside edge of the surrogate pit during a hydrotest. The x-rays used to image the implosion were generated with the 15-MeV electron beam from the betatron borrowed from the University of Illinois. The detector consisted of a lead glass converter and a Wilson cloud chamber to detect the recoil electrons. The dark area in each image is the shadow cast by the pit. The radius of the pit is smaller in the right image.

Figure 3. The Radiolanthanum Experiments
This photo taken at Los Alamos during the Manhattan Project shows the "remote handling" of a kilocurie source of radiolanthanum located inside a lead container. This strong gamma-ray source would be placed at the center of a hydrotest assembly to measure the areal density of the pit (from the center outward) as a function of time.

waves from each detonation point to cancel each other out upon interaction, creating the desired converging detonation wave. The results were disappointing. The recovered ball of metal had been compressed but showed many asymmetries. Later experiments with multiple points of detonation around a cylindrical shell showed that high pressure develops where the detonation waves collide, which could result in the formation of "jets." The group then modified commercial x-ray machines to achieve precision timing of the x-ray flashes to about 1 microsecond so that the x-ray flashes could be coordinated with the explosive shots. Indeed, the resulting images confirmed that jets did form at the interaction between multiple detonation waves. That diagnosis led to the design of explosive "lenses," which shape the individual detonation waves so that such high-pressure areas do not form. Flash radiography of small imploding metallic spheres revealed two other reasons for nonideal implosion: density variations in the explosives and asynchrony among the individual detonators. These discoveries led to improvements in the manufacture of explosives and to "electric detonation" for more reliable timing.

To interrogate implosion of a full-scale device (with a surrogate pit material), they would need more penetrating radiation—x-ray photons with energies near 4.0 MeV. Oppenheimer decided to acquire the University of Illinois betatron, an electron accelerator that produced 1-microsecond-long pulses of 15-MeV electrons. As already discussed, the high-energy electrons produced bremsstrahlung radiation as they passed through a high-Z target. The high-energy photons produced by the betatron penetrated the high explosive of a full-scale device but were stopped by the large areal density of the pit itself; therefore, a "shadow" of the pit's outer contour could be observed by detection of the photons that made it through the device. These photons were detected when a sheet of lead glass was placed on the other side of the device. Interactions of x-rays with the atomic electrons in the lead glass produced energetic recoil electrons, and those recoil electrons made visible tracks in a vertical cloud chamber. That system provided the first flash radiograph of an "integrated" test (see Figure 2). The work on flash x-ray

imaging of full-scale devices was said to be "among the most impressive of several such achievements at Los Alamos" (Hawkins 1961).

After developing techniques to diagnose symmetric implosions, the Manhattan project pioneers wanted to measure what was happening inside the pit. For that purpose, they placed a small capsule of the radioactive isotope lanthanum-140 at the center of the pit. As the high explosive compressed the pit, the 1.46-MeV photons from the decay of the lanthanum-140 penetrated through to the outside of the pit, and their intensity was measured as a function of time. Those data provided a measure of the areal density of the pit as a function of time. Although the experiments were effective, the environmental hazards (see Figure 3) of both their production and their aftermath resulted in abandonment of the program in 1962.

Figure 4. A PHERMEX Shot
This photo shows an explosive shot at PHERMEX. The high-energy pulsed x-ray machine has served the weapons program for 40 years.

PHERMEX

The Los Alamos facility known as PHERMEX (for pulsed high-energy radiographic machine emitting x-rays) was commissioned in 1963 (see Figure 4). It was the first of a new generation of flash x-ray machines designed to produce enough flux to penetrate the center of a hydrotest experiment at "nuclear" time. The design of this high-energy pulsed x-ray machine, including techniques for recording the images, was the culmination of extensive Los Alamos studies led by Doug Venable and completed in the early 1950s.

Those studies defined the dose needed to penetrate the center of a hydrotest assembly and the feasibility of getting good images of the less-dense parts of the assembly. It was shown that systems up to 4 λ in thickness could be imaged on film detectors. For objects up to 10 λ in thickness, the large background of scattered radiation would obscure the film images.

The studies were performed on static test objects that had been stretched in the beam direction to have areal densities commensurate with the high volume densities reached during hydrotest implosions. The doses needed to measure the internal densities of those test objects were determined as a function of scale. The idea was that, although PHERMEX could not see through a full-scale device, the hydrodynamics could be studied at quarter or half scale with surrogate materials. To minimize the obscuring effects of scattered x-rays in the thickest regions, the objects were radiographed through a graded collimator designed to be an approximate inverse of the object. Graded collimation dramatically reduced the scattered background while still allowing the thinner parts of the object to be seen. This technique has been crucial in enabling radiography across the full range of configurations reached during hydrotests.

At PHERMEX, three very large 50-megahertz radio-frequency (rf) resonators provide the energy needed to accelerate short pulses of electrons totaling 9 microcoulombs of electric charge to 30 MeV. Those pulses are then directed at a high-Z target to produce x-rays. When PHERMEX was commissioned, it produced 200-nanosecond-long pulses of x-rays exceeding 9 roentgens at 1 meter from the production target.

Thousands of experiments have been performed at the facility, including small-scale experiments to develop the physics of high-explosive-driven systems (see Figures 5 and 6), and a large number of major hydrotests. Much of this work has been compiled and presented in a marvelous summary of shock physics (Mader et al. 1980). PHERMEX has also undergone many upgrades during its lifetime. Currently, it can produce a single 200-nanosecond-long pulse with a spot size of 3 millimeters and a dose of 400 roentgens at a distance of 1 meter from the target, more than 40 times the

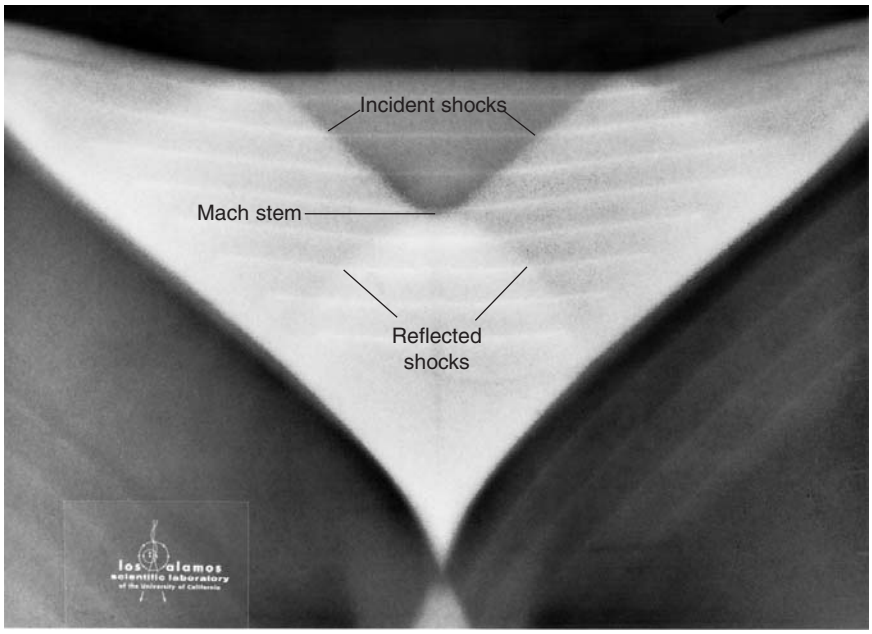

Figure 5. PHERMEX Radiograph of Hydrodynamic Flow
Dating from the late 1960s, this radiograph shows colliding shock waves in aluminum. The horizontal lines are thin foils of high-density metal interspersed in the aluminum to indicate the material flow. A Mach stem has formed at the intersection of the shock waves.

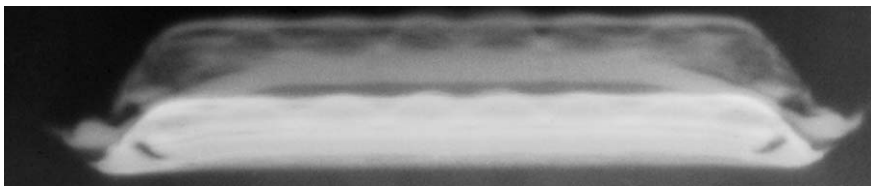

Figure 6. Double-Pulse PHERMEX Radiograph of Spall in Iron
An iron plate is driven by an explosive initiated at a number of individual points. The iron has spalled into a series of layers, and the effects of the initiation points are apparent. Successive transmission of two short x-ray pulses produces two sequential images on one film.

dose provided when it was commissioned.

For most of PHERMEX's history, a technique known as screen-enhanced film has been used to record images of the experiments performed in front of the facility. That is, the transmitted x-rays are converted through Compton scattering into moving electrons in a millimeter-thick sheet of lead. Then, as the electrons slow down in the sensitive photographic film located behind the lead sheet, their tracks are recorded (see Figure 1). Recently, active cameras have been developed and fielded. They have higher sensitivity, higher quantum efficiency, and wider linear dynamic range than film. The latest version of these active cameras can take up to four sequential images and thereby tap the two-pulse capability of PHERMEX. For the first time, we can get high-quality images for each individual pulse (See the article "The DARHT Camera" on page 92.)

Ultimately, the amount of charge (number of electrons) delivered by PHERMEX, and in turn, the x-ray dose, are limited by the stored energy in the rf resonators. The voltage in the resonators decreases as energy is transferred to the beam; the resulting spread in beam energy at high electron current leads to an unacceptably large spot size on the x-ray production target. Also, high-explosive-driven experiments generate material velocities in the range of several millimeters per microsecond (mm/μs). Thus, the material moves appreciably during the length of the typical 200-nanosecond-long x-ray pulse. Reducing this "motion blur" to levels that do not interfere with the interpretation of the experiment requires pulse lengths of about 100 nanoseconds or less. In spite of the limitations in dose and pulse length, PHERMEX has been a workhorse for the weapons program during the 40 years of its operation.

The DARHT Facility

A recent review (Ekdahl 2002) of the current state of electron accelerators for flash radiography reports that the United States, the United Kingdom, and France are all developing new flash-radiography capabilities to meet the challenges of maintaining nuclear weapons stockpiles under the restrictions of a moratorium on nuclear tests. This new generation of machines is designed to provide higher doses, better position resolution, shorter pulse lengths, and in some cases, data from a single experiment taken at multiple times and along multiple axes, so that the time-dependence and three-dimensional (3-D) aspects of an implosion can be elucidated.

As early as 1968, Doug Venable had proposed adding a second x-ray axis to PHERMEX, perpendicular to the first, to allow orthogonal tomography. And in 1981, long before the moratorium on testing, John Hopson and Tim Neal presented the first con-

(a)

(b)

Figure 7. The DARHT Facility
(a) The DARHT facility houses two linear induction accelerators set at right angles to each other and focused on a single firing point. (b) Each accelerator consists of a row of induction cells, each coupled to its own energy-storage device. The pulsed-power machine accelerates very large (kiloampere) electron currents, which produce very intense x-ray pulses that are 60 ns long.

cept for the DARHT facility at Los Alamos. It would be built at a new firing site and use two high-dose pulsed-power machines to provide orthogonal x-ray views of a single hydrotest, a capability similar to that at the Atomic Weapons Establishment (AWE) in Aldermaston, England.

The linear induction accelerator (LIA), rather than the pulsed-power diode machines originally proposed, is the technology being used for the two flash-radiography machines at DARHT (see Figure 7). LIAs were pioneered for flash radiography at Lawrence Livermore National Laboratory in the 1980s. Their operating principle is similar to the betatron technology used for the first high-energy flash radiography in Los Alamos in the sense that stored energy from a pulsed-power system is inductively coupled to a high-current electron beam. But in the LIA, the coupling is accomplished by a row of many induction cells rather than a single transformer. Because there are many transformers, each coupled to its own external energy-storage device, the electron currents can be much larger than the limiting currents at PHERMEX. In fact, kiloampere electron currents can be readily accelerated in an LIA.

One performance feature to help rank machines that produce different x-ray spot sizes and doses is the root-square-mean (rms) error with which the radiographs from each machine can be used to determine the position of a material interface. This rms error is inversely proportional to the square root of the dose d and proportional to the radiographic position resolution Δx. Charlie Martin of AWE proposed the simple radiographic figure of merit $\text{FOM} = d/\Delta x^2$. The position resolution includes contribution from the x-ray spot size, the pulse length (which produces motion blur), and the detector resolution. The machine design determines the first two of these.

The first axis of DARHT, which has already been used for hydrotests, has delivered a dose of 500 roentgens in a 60-nanosecond-long pulse over a 2-milllimeter spot. For the same pulse length, PHERMEX can provide a dose of only 120 roentgens in a spot of 3 millimeters. These performance parameters indicate that DARHT achieves about an order-of-magnitude improvement over PHERMEX in terms of Martin's radiographic figure of merit. The second axis of DARHT accelerated its first beam to full energy at the end of 2002 and will soon provide pulses with dose and spot size similar to those produced by the first axis. The new feature of this second axis is the production of four such pulses in 2 microseconds. That capability should be available to interrogate hydrotests by the end of 2005.

The first axis of DARHT is already providing weapons scientists with the clearest views ever seen of the inside of a hydrotest. The hydrodynamic data from those tests are used to validate new physics models that are being incorporated into weapons codes. Once the second axis becomes available, scientists will take four sequential radiographs along one axis and one radiograph along the perpendicular axis, thus providing the very first 3-D data from a single U.S. hydrotest.

Figure 8 compares radiographs of the unclassified FTO (refer to Figure 1) taken at PHERMEX in the late 1980s and at the first axis of DARHT. The FTO was designed to compare the performance of flash x-ray machines. The DARHT system—the combination of x-ray source and detectors—clearly demonstrates a very dramatic increase in performance. This facility is expected to be the centerpiece of the nation's hydrotest program for at least a decade.

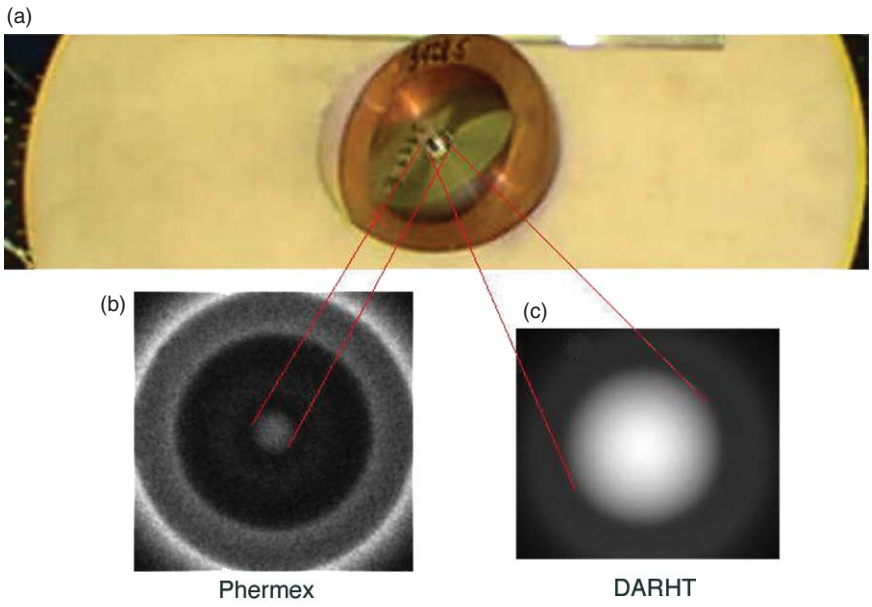

Figure 8. A Comparison of X-Radiographs from DARHT and PHERMEX
A photograph of half of the FTO is shown in (a), a radiograph of the FTO from PHERMEX is shown in (b), and another radiograph of the FTO from DARHT is shown in (c). The DARHT image reveals a dramatic improvement in quality caused by an improved source and better detector. The PHERMEX radiograph was taken with a graded collimator, whereas the DARHT radiograph was taken with a small, field-of-view, rough collimator, imaging less of the object with lower background. The boxes outline the approximate field of view of each of the radiographs. Comparing these radiographs with the early radiograph in Figure 2 reveals the progress made in flash x-ray radiography since the Manhattan Project .

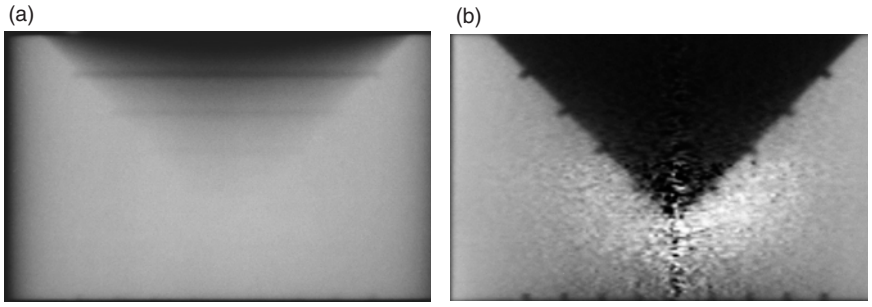

Figure 9. Improvements in Data Analysis
(a) The radiograph of a steel cylinder with a diameter of 12 cm was taken with a cobalt-60 source. The cylinder has a conical section machined out of the top. Square grooves (2 mm by 2 mm) were machined at the bottom of the cylinder and on the inner surface of the conical section to assess the quality of the radiograph and subsequent image processing. (b) The reconstruction process, which first extracts the areal density and eventually the volume density of the cylinder, makes readily apparent many of the grooves that were almost invisible in the original radiograph. The enhanced noise at the center of the cylinder is an unavoidable consequence of this process. The reconstruction process was first implemented in the 1980s.

Detectors, Collimators, and Data Analysis

The x-ray dose and spot size produced in state-of-the-art multipulse x-ray machines are limited by interactions between the electron beam and the high-*Z* target. When an electron beam carrying thousands of amperes interacts with an x-ray production target, it creates a high-density plasma of ionized target material and surface impurities. The electrons then interact with the plasma, dynamically changing the effective focal point and increasing the spot size. In addition, the beam causes material at the surface of the target to spall, which reduces the target thickness and, in turn, reduces the dose as a function of time. Both the destruction of the target and the beam-plasma interactions make the goal of multipulse high-dose x-ray radiography difficult to attain. Some progress is being made in techniques to mitigate these problems, but so far, improvements have been only incremental.

Difficulties inherent in increasing the dose have led researchers to search for optimal ways to extract the maximum information from the available doses. They have adopted and extended techniques first investigated at PHERMEX: graded collimation, advanced data analysis, image plate detectors, and multiframe active cameras. More sensitive detectors allow measurements to be made with less incident dose. Large-scale Monte Carlo calculations have led to improved experimental designs that increase signal-to-noise ratio by reducing scattered background. New data-analysis techniques have led to optimally estimating features of interest (refer to Figure 9). These advances in experimental design, detectors, and data analysis have been as important as the increased power and resolution of the x-ray beams for increasing the information that weapons scientists obtain from flash radiography.

Proton Radiography

In spite of numerous improvements in high-energy flash radiography over the past 50 years, the dose limitations, position resolution, and backgrounds still limit the utility of the technology for obtaining adequate quantitative information from hydrotests for stockpile certification. Recently, a new idea, lens-focused proton radiography, has provided a potential solution to these problems.

As described earlier, electromagnetic scattering processes limit the maximum interaction length of an x-ray to a value far from the optimum for hydrotest experiments. Hadronic probes provide an alternative. Hadrons are fundamental particles, such as neutrons and protons, that interact with matter through the strong (nuclear) force. The absorption cross section, σ_A, for the strong interaction of hadrons with a nucleus with mass number A can be approximated as

$$\sigma_A = \pi r_A^2 \ , \qquad (7)$$

which is the geometric cross section of the nucleus, where $r_A \approx 1.3A^{1/3}$ femtometers. (A Fermi, or femtometer, is 10^{-15} meter.) This absorption cross section implies that the mean free path, $\lambda^* = 1/n\sigma$ (where n is the number density of atoms), for a hadron in uranium of nominal density is a length of about 10 centimeters, or an interaction length of 200 gm/cm^2, an order of magnitude larger than that of high-energy x-rays. This interaction length is almost perfectly matched to hydrotest radiography. Consequently, a much lower incident flux of hadrons will produce the same statistical information now obtained from a higher flux of high-energy x-rays.

Of course, protons are charged, and therefore, when they interact with matter, the Coulomb force between the protons and the charge of the electrons and the nuclei in the material causes the protons to continuously slow down and scatter into other directions. However, for a proton with high enough energy, electromagnetic scattering processes produce only small changes in its direction and energy, even when it traverses a significant thickness of material. Thus, nuclear inelastic scattering remains the dominant mechanism removing protons from an incident high-energy proton beam. Consequently, high-energy protons have a large interaction length and are interesting as a radiographic probe. Moreover, current accelerators routinely produce high-intensity, short pulses of high-energy protons.

Focusing Protons. The charge on the proton allows using magnetic lenses to focus a proton beam of a selected energy or momentum (the two are almost equivalent at high energies, hundreds of times above the rest mass energy of the proton, which is 938.272 MeV). This focusing capability gives great flexibility to proton radiography and leads to many advantages over the standard point-source x-radiography shown in Figure 1.

Figure 10 shows the proton radiography line at LANSCE, which has four separate lenses: an angle matching lens (not shown), consisting of three quadrupole magnets, and three imaging lenses, each consisting of four quadrupole magnets. The initial beam goes through the angle-matching lens, which is tuned to focus the protons of a selected initial momentum P_i onto image plane 0 such that the protons (black rays) are spread over an area equal to that of the object and each proton's directional angles relative to the beam axis along the z-direction (θ_i in the x-z plane and ϕ_i in the y-z plane) are proportional to its distance from the beam axis, that is, $\theta_i = Ax_i$ and $\phi_i = -Ay_i$. To calibrate our experiment, we measure the beam intensity at selected points on image plane 0. Lens 0 then refocuses the protons to have the same position–angle correlation at the object plane that they have at image plane 0, just inverted from plane 0 to the object plane. Protons transmitted through the object are scattered by Coulomb forces into a cone of angles about their initial directions (represented by the red and blue rays). Even though the transmitted protons now have a spread in momentum, lens 1 can refocus the beam onto image plane 1 because the lens is designed to cancel the leading chromatic aberrations (the changes in image position caused by variations in momentum). A collimator in lens 1, like the f-stop of a conventional camera, selects the range of proton angles that can be transmitted to image plane 1. The contrast of the image can be increased by selection of a collimator that cuts into the Coulomb scattering cone.

Correcting Chromatic Aberrations. The largest aberration in the lens system is chromatic, or momentum dependent. That is, protons whose momentum varies from that for which the magnetic lens is tuned are the leading cause of image blurring. The angle-matching lens has been designed so that the proton trajectories incident at the object plane have a position–angle correlation that minimizes the chromatic aberration in the imaging lenses. In particular, that position–angle correlation at the object plane is such that the largest chromatic aberrations in image position cancel each other—the aberration proportional to θ_i cancels the one proportional to x_i, and the aberration proportional to ϕ_i cancels the one proportional to y_i.

High-Efficiency Detection. Protons are detected with high efficiency when a thin sheet of scintillator is placed at the image plane. As the protons pass through, the scintillator emits enough light for an image to be stored in a gated charge-coupled device camera, but it does not perturb

(a)

(b)

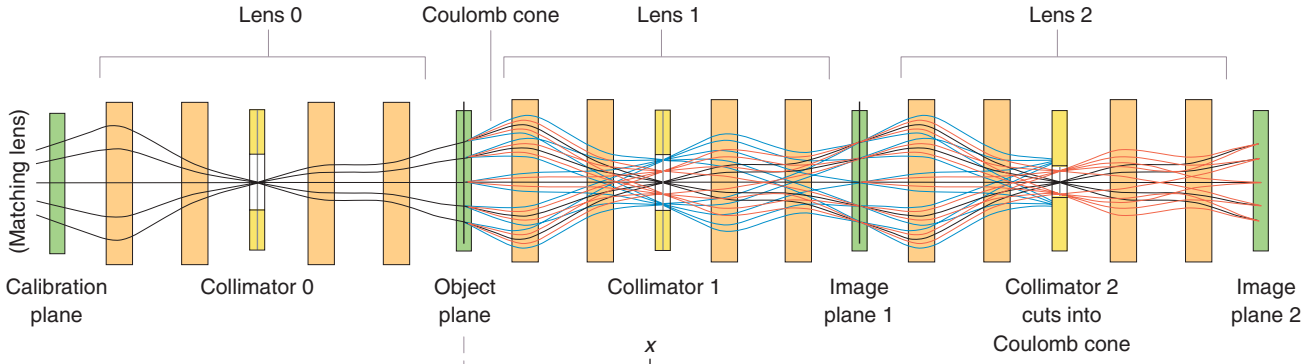

(c)

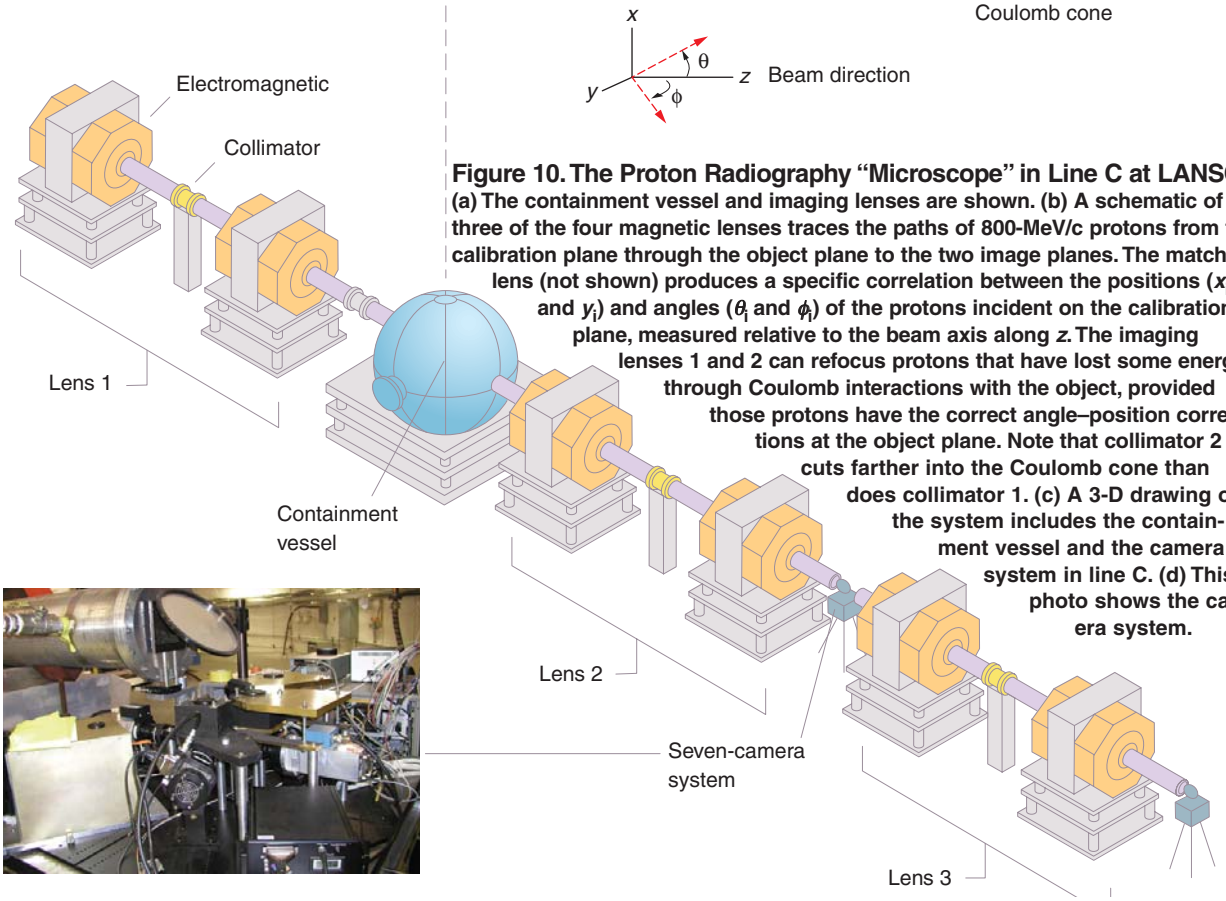

(d)

Figure 10. The Proton Radiography "Microscope" in Line C at LANSCE
(a) The containment vessel and imaging lenses are shown. (b) A schematic of three of the four magnetic lenses traces the paths of 800-MeV/c protons from the calibration plane through the object plane to the two image planes. The matching lens (not shown) produces a specific correlation between the positions (x_i and y_i) and angles (θ_i and ϕ_i) of the protons incident on the calibration plane, measured relative to the beam axis along z. The imaging lenses 1 and 2 can refocus protons that have lost some energy through Coulomb interactions with the object, provided those protons have the correct angle–position correlations at the object plane. Note that collimator 2 cuts farther into the Coulomb cone than does collimator 1. (c) A 3-D drawing of the system includes the containment vessel and the camera system in line C. (d) This photo shows the camera system.

the proton beam significantly. In fact, so few protons are absorbed that the same pulse can be reimaged by lens 3. Lens 3 has a smaller collimator than lens 2 to cut farther into the Coulomb scattering cone (note that the blue rays are blocked). Since Coulomb scattering depends on the Z-number of the material, this double imaging process enables material identification from proton radiographs.

The ability to refocus protons means that the closest detector (image plane 1) can be at a long standoff distance from the blast. That characteristic, combined with the momentum selectivity of the lens, results in much lower backgrounds in proton radiography than in x-ray radiography. As a result, the need for background mitigation techniques such as graded collimation, an essential part of x-ray experiments, is eliminated. The combination of lower backgrounds and energy-independent cross sections allows a new level of precision not available in x-radiography.

Proton radiography is being studied with the 800-MeV/c proton beam provided by the LANSCE accelerator and with a 24,000-MeV beam provided by the alternating gradient synchrotron (AGS) at Brookhaven National Laboratory.

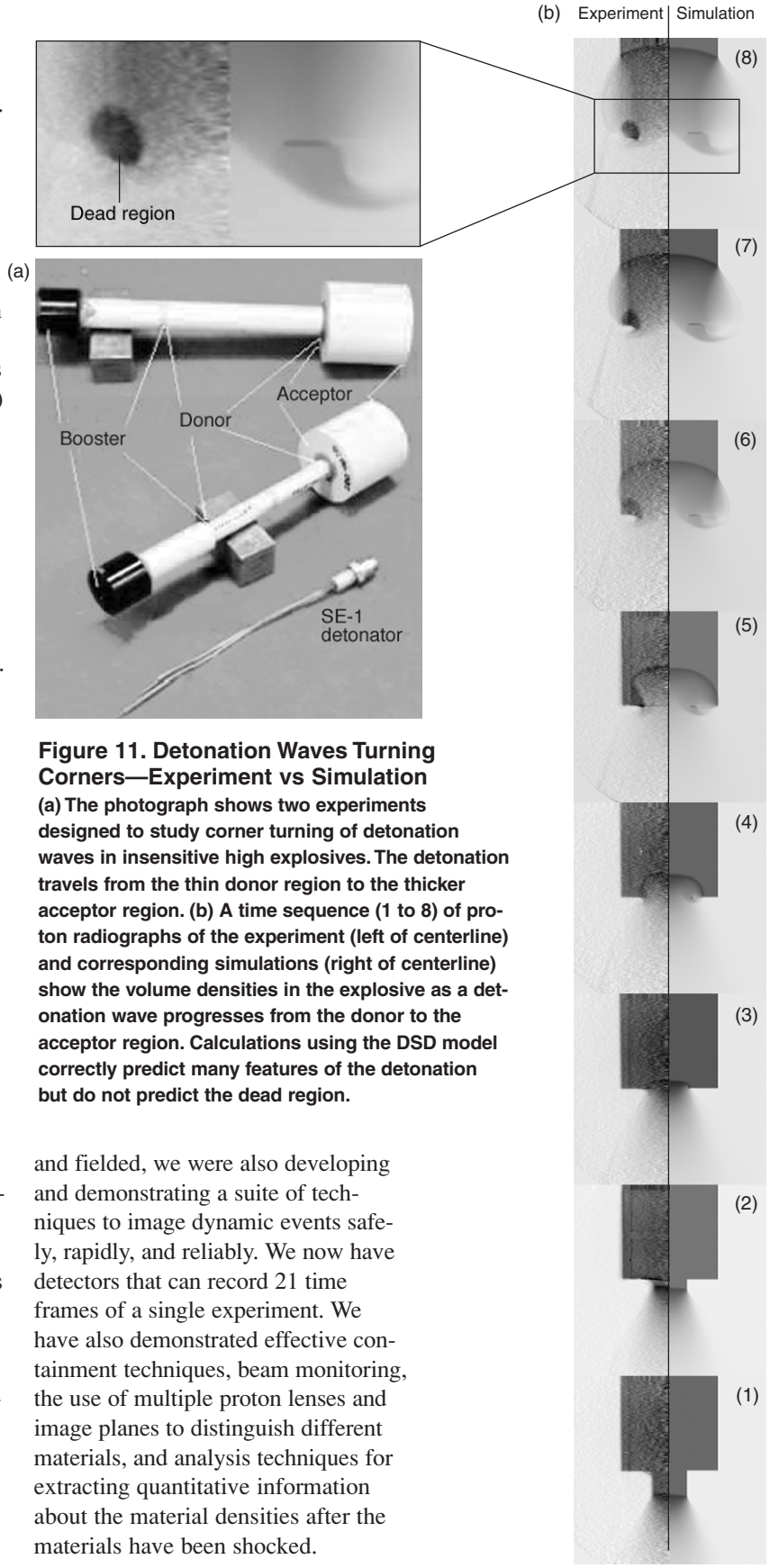

Figure 11. Detonation Waves Turning Corners—Experiment vs Simulation

(a) The photograph shows two experiments designed to study corner turning of detonation waves in insensitive high explosives. The detonation travels from the thin donor region to the thicker acceptor region. (b) A time sequence (1 to 8) of proton radiographs of the experiment (left of centerline) and corresponding simulations (right of centerline) show the volume densities in the explosive as a detonation wave progresses from the donor to the acceptor region. Calculations using the DSD model correctly predict many features of the detonation but do not predict the dead region.

Studies at LANSCE

On average, about 40 small-scale dynamic experiments are being performed each year at the proton "microscope" in line C at LANSCE (refer to Figure 10). Each experiment (or physics package) uses up to 10 pounds of high explosive. The physics package is contained in a vessel shown in Figure 10(c). These experiments are designed to study high-explosive detonation and dynamic material failure and to perform small integral tests to validate the models used in weapons codes. At the time that the first experiments were being planned, designed, and fielded, we were also developing and demonstrating a suite of techniques to image dynamic events safely, rapidly, and reliably. We now have detectors that can record 21 time frames of a single experiment. We have also demonstrated effective containment techniques, beam monitoring, the use of multiple proton lenses and image planes to distinguish different materials, and analysis techniques for extracting quantitative information about the material densities after the materials have been shocked.

As an example, Figure 11 illustrates the experimental setup, the data, and the detonation shock dynamics (DSD) simulations of a set of experiments to study the corner turning of a detonation front in the high explosive PBX 9502. This insensitive, plastic-bonded material has been incorporated in some systems in the nuclear weapons stockpile to increase safety because it was specifically designed to be hard to detonate. The downside is that detonation waves do not propagate as well in PBX 9502 as they do in conventional high explosives. As a result, when the geometry of the explosive forces the detonation wave to turn a corner, dead zones (regions that do not detonate) appear.

During the experiment, a detonation wave is launched in a cylindrical stalk of PBX 9502 by a booster, and a sequence of proton radiographs is taken as the detonation wave propagates into a cylinder with a larger diameter. Figure 11(b) shows a frame-by-frame comparison of radiographs (left) and the corresponding simulations (right) for that sequence. The proton radiographs show that a dead region (dark) of unburnt explosive in the shape of a doughnut remains after the detonation wave expands in the larger cylinder. This phenomenon is not yet captured in the DSD model (the DSD model is presented in the article "High Explosives Performance" on page 96). The experimental data guide the development of models aimed at better predictions of this phenomenon.

The 800-MeV/c proton beam at line C has also been used to radiograph materials as they break apart, or spall, under the influence of high strain rates. Figure 12 shows proton radiographs of a half cylinder of titanium driven by the detonation of an embedded half cylinder of high explosive. The rapid propagation of the high-pressure detonation wave down the high-explosive half cylinder produces very high strain rates in the titanium. As a result, the metal expands much more before failing than it would if it had been slowly stretched. The cracks and voids that develop as the metal expands are readily apparent in the inset. The new models needed to describe this behavior are being developed, and proton radiography provides data that help in this effort.

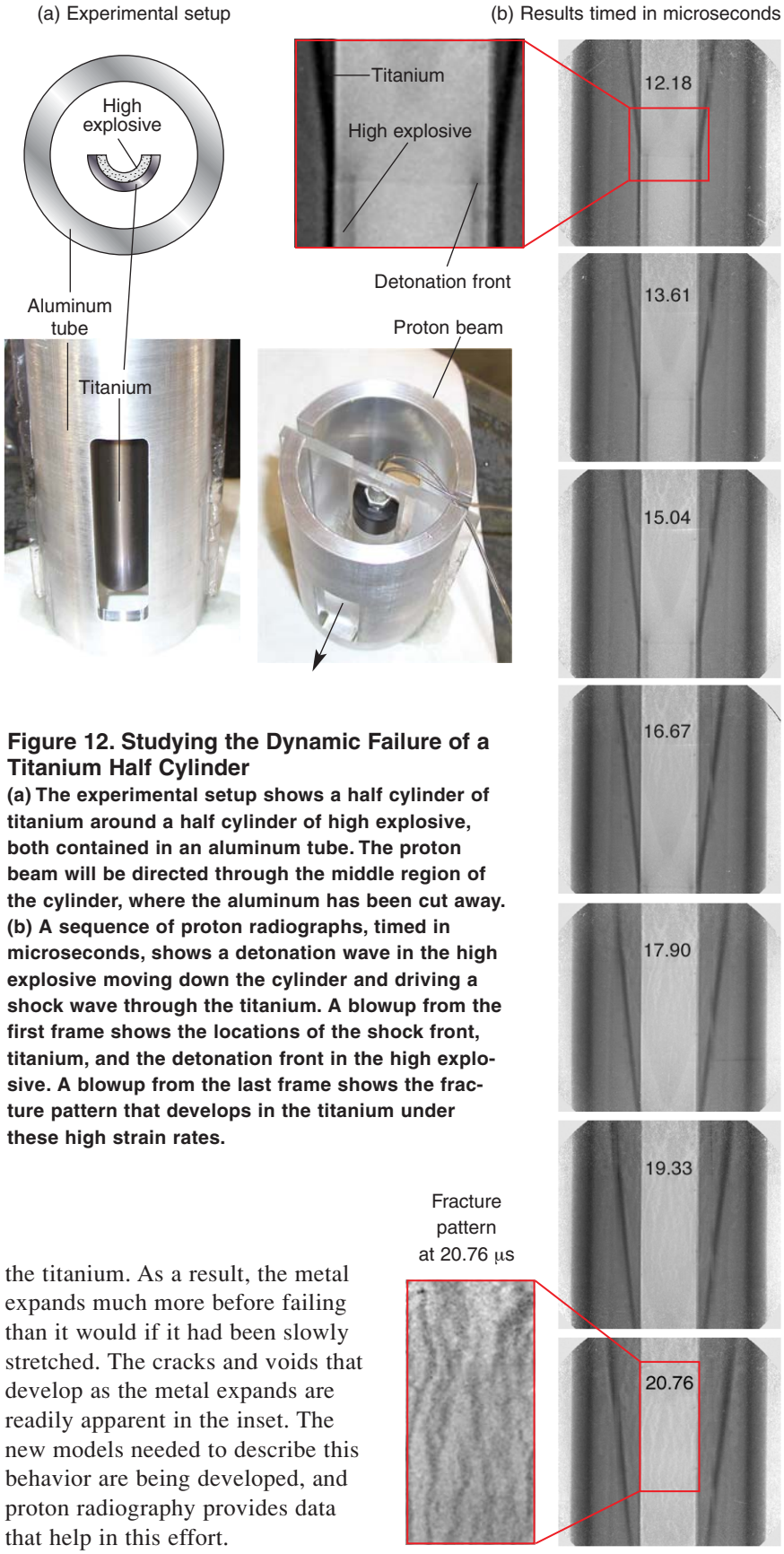

Figure 12. Studying the Dynamic Failure of a Titanium Half Cylinder
(a) The experimental setup shows a half cylinder of titanium around a half cylinder of high explosive, both contained in an aluminum tube. The proton beam will be directed through the middle region of the cylinder, where the aluminum has been cut away. (b) A sequence of proton radiographs, timed in microseconds, shows a detonation wave in the high explosive moving down the cylinder and driving a shock wave through the titanium. A blowup from the first frame shows the locations of the shock front, titanium, and the detonation front in the high explosive. A blowup from the last frame shows the fracture pattern that develops in the titanium under these high strain rates.

High-Energy Proton Radiography

The experiments with the 800-MeV/c proton beam at LANSCE have been immensely valuable in demonstrating and developing proton radiography. For radiographs of the much higher areal densities involved in full-scale hydrotests, a higher-energy proton beam is required. We have conducted studies using high-energy proton beams that have exactly the format (beam size and intensity) needed to perform flash radiography for full-scale hydrotests.

Our first higher-energy experiments at AGS used secondary protons (whose energy is lower than that of the main beam), which are produced at very low rates. Although the exposures lasted for several hours, these first radiographs of the FTO, made with a quadrupole lens, showed great potential for the technique. In more recent experiments, we used a fast-extracted high-energy beam (30-nanosecond-long pulses) of up to 10^{11} protons from the accelerator to radiograph various static test objects and to develop techniques for quantitative analysis of dynamic experiments.

Figure 13 shows the dramatic improvement in FTO radiographs obtained at the AGS. These experiments have demonstrated low backgrounds, multiple views, good statistics, and quantitative precision. We have also compared proton and x-ray radiography by radiographing the same thick, classified test object with the first axis of DARHT and with the high-energy proton beam at AGS. The results of this classified experiment demonstrate the dramatic improvement in the quality of radiography expected from this new probe.

Material identification has also been demonstrated for static experiments at the AGS in experiment 933. Material identification would be valuable in studying the properties of material interfaces in hydrotests, but moving objects present some new difficulties that must be studied. We are developing Monte Carlo simulation codes to study the properties of the entire beam line, including the effects of test objects with complicated geometries.

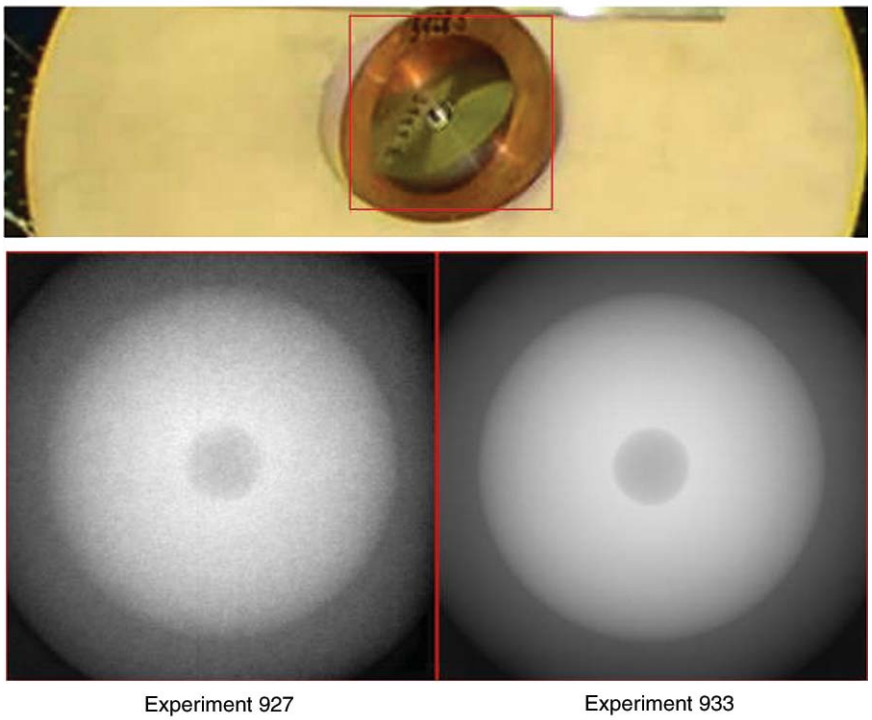

Figure 13. Proton Radiographs of the FTO
The radiograph on the left was recorded in a 4-h exposure in a secondary beam with about 10^9 protons with an energy of 10 GeV in energy. The radiograph on the right was made in a 40-ns exposure with about 2×10^{10} protons with an energy of 24 GeV.

Very recently, we conducted another series of experiments at the AGS on static test objects. These experiments were designed to allow assessing the quantitative accuracy of proton radiography for the study of criticality and mix, effects that are of the highest possible importance to stockpile stewardship. The test objects were carefully crafted to provide unprecedented fidelity to weapon design calculations. Some of the test objects constituted a weapon implosion "time-series," reflecting very precisely the microsecond-timescale changes in device configuration that the design calculations predict.

Another aim of the recent experiments was to demonstrate a capability to study mix and other stewardship-relevant phenomena in dynamic experiments at the AGS. Although the recent experiments used only static test objects, they were designed to pave the way for future experiments that would incorporate high explosives and be fielded in containment vessels. Even though a far cry from weapons hydrotests, these dynamic experiments would both provide unique data on hydrodynamic performance needed for the stewardship program and demonstrate that this type of imaging is fully compatible with the technology and infrastructure needed in the hydrotest regime—including, of course, processes and procedures required for the protection of the environment, personal safety, and health.

The success of proton radiography

has led Los Alamos to propose a new facility for hydrodynamic testing. The new proton-radiography facility will be used to make detailed quantitative movies of hydrotests that capture with unprecedented precision the time development of an implosion.

Summary

Penetrating flash radiography has provided critical information to weapons designers since the inception of the Manhattan Project. Radiographic machines used during that time provided images of the outer pit surface to calibrate numerical models of the hydrodynamic performance of the device. Radiography was also used to identify several important early problems with the implosion device—for example, interaction of the high-explosive waves that caused jetting of the heavy metal. PHERMEX, commissioned nearly 40 years ago, provided the first radiographic machine capable of obtaining detailed data on the density distributions at the center of a primary in a radiographic hydrotest. In the intervening 40 years, there has been tremendous progress in x-ray machine and detector performance, scatter reduction, and quantitative analysis of flash x-ray radiography for stockpile stewardship. The second axis of DARHT, soon to be commissioned, will complete a state-of-the-art facility that will provide weapons designers with their clearest views of the inside of a hydrotest ever obtained.

Both PHERMEX and DARHT represented quantum leaps forward in our ability to peer inside implosions of mock nuclear weapon systems. However, the ultimate goal to produce highly quantitative, 3-D, time-evolving density maps, needed for certification without testing, has still not been reached. In the future, it is likely that new radiographic machines with improved performance will be needed to certify the enduring stockpile. The recent invention of proton radiography at Los Alamos has the potential to meet this future need. Experiments have shown that proton radiography can provide high-quality radiographic information at many times during dynamic experiments using the 800-MeV/c proton beam from LANSCE. Experiments performed with the higher energy 24,000-MeV/c proton beam from the AGS accelerator have demonstrated low backgrounds, small statistical errors, and well-controlled systematic uncertainties. The combination of high-quality radiography, small-scale experimentation, and predictive modeling can form the foundation of a robust stockpile stewardship program without underground testing. Interestingly, more primitive versions of the same tools formed the design basis for the successful Trinity test in 1945. ■

Acknowledgments

We are grateful for the time Doug Venable, John Hopson, and Tim Neal spent with us describing the history of PHERMEX and DARHT. Susan Seestrom's early editing was a great help in allowing us to get to a final manuscript. The Reports Library, Copy Center, and photo archive were invaluable resources for delving into the early history of flash radiography at the Laboratory. We would also like to thank Tim Neal, John Zumbro, Stephen Sterbenz, and Ken Hanson for contributing materials and providing helpful advice.

Further Reading

Anthouard, P., J. Bardy, C. Bonnafond, P. Delsart, A. Devin, P. Eyharts et al. 1998. AIRIX Prototype Technological Results at CESTA. In *Proceedings of the 1997 Particle Accelerator Conference*. (Vancouver, B. C., Canada, May 12–16, 1997). Vol. 1, p. 1254. Edited by M. Comyn, M. K. Craddock, M. Reiserr, and J. Thomson. Piscataway, New Jersey: IEEE.

Alrick, K. R., K. L. Buescher, D. J. Clark, C. J. Espinoza, J. J. Gomez, N. T. Gray et al. 2000. "Some Preliminary Results From Experiment 933." Los Alamos National Laboratory document LA-UR-00-4796.

Beer, A. 1852. Bestimmung der Absorption des Rothen Lichts in Farbigen F1üssigkeiten. *Ann. Phys. Chem.* **86**: 78.

Boyd, T. J. 1967. "PHERMEX: A Pulsed High-Energy Radiographic Machine Emitting X-Rays." Los Alamos Scientific Laboratory report LA-3241.

Burns, M. J., B. E. Carlston, T. J. T. Kwan, D. C. Moir, D. S. Prono, S. A. Watson et al. 1999. DARHT Accelerators Update and Plans for Initial Operation. In *Proceedings of the IEEE Particle Accelerator Conference*. (The 18th Biennial Particle Accelerator Conference, New York, March 27–April 2, 1999). Vol. 1, p. 617. Piscataway, New Jersey: IEEE.

Christofilos, N. C., R. E. Hester, W. A. S. Lamb, D. D. Reagan, W. A. Sherwood, and R. E. Wright. 1964. High-Current Linear-Induction Accelerator for Electrons. *Rev. Sci. Instrum.* **35** (7): 886.

Ekdahl, C. 2002. Modern Electron Accelerators for Radiography. *IEEE Trans. Plasma Sci.* **30** (1): 254.

Eyharts, P., P. Anthouard, J. Bardy, C. Bonnafond, P. Delsart, A. Devin et al. 1998. Beam Transport and Characterization on AIRIX Prototype at CESTA. In *Proceedings of the 1997 Particle Accelerator Conference*. (Vancouver, B. C., Canada, May 12–16, 1997). Vol. 1, p. 1257. Edited by M. Comyn, M. K. Craddock, M. Reiserr, and J. Thomson. Piscataway, New Jersey: IEEE.

Ferm, E. N., C. L. Morris, J. P. Quintana, P. Pazuchanics, H.L. Stacy, J. D. Zumbro et al. 2002. Proton Radiography Examination of Unburned Regions in PBX 9502 Corner Turning Experiments. *AIP Conference Proceedings* **620** (1): 966.

Goldsack, T. J., T. F. Bryant, P. F. Beech, S. G. Clough, G. M. Cooper, R. Davitt, and R. D. Edwards. 2002. Multimegavolt Multiaxis High-Resolution Flash X-Ray Source Development for a New Hydrodynamics Research Facility at AWE Aldermaston. *IEEE Trans. Plasma Sci.* **30** (1): 239.

Hawkins, D. 1961 (written 1946). "Los Alamos Scientific Laboratory—Manhattan District History, Project Y, the Los Alamos Project." Los Alamos Scientific Laboratory report LAMS-2532 (Vol. I).

Hoddeson, L., P. W. Henriksen, R. A. Meade, and C. Westfall. 1993. Critical Assembly—A Technical History of Los Alamos during the Oppenheimer Years, 1943–1945. Cambridge: Cambridge University Press.

Kwan, T. J. T., C. M. Snell, and P. J. Christenson. 2000. Electron Beam–Target Interaction and Spot Size Stabilization in Flash X-Ray Radiography. *Phys. Plasmas* **7** (5): 2215.

Mader, C. L., T. R. Neal, and R. D. Dick. 1980. *LASL PHERMEX Data*, Vol. I. Berkeley: University of California Press.

Mueller, K. H. 1985. Collimation Techniques for Dense Object Flash Radiography. *Proc. Soc. of Photo-Optical Instrumentation Engineers* **491** (1) :130.

Morris, C. L. et al. Defense Review LACP-02-89 (to be published 2003).

Neddermeyer, S., and A. R. Sayer. 1946. "Betatron Cloud-Chamber Studies with Levitated Assemblies." Los Alamos Scientific Laboratory report LA-483.

Röntgen, W. C. 1896. On a New Kind of Rays. *Nature* **53:** 274.

Venable, D. 1964. PHERMEX. *Phys. Today* **17** (12):19.

Watson, S., T. Kauppila, L. Morrison, and C. Vecere. 1997. The Pulsed High-Energy Radiographic Machine Emitting X-Rays (PHERMEX) Flash Radiographic Camera. In *SPIE 22nd International Congress on High-Speed Photography and Photonics*. (International Congress on High Speed Photography and Photonics, Santa Fe, New Mexico, October 27–November 1, 1996). Edited by D. L. Paisley, and A. M. Frank. Vol. 2869, p. 920. Bellingham, Washington: SPIE.

For further information, contact Gregory Cunningham (505) 667-2562 (cunning@lanl.gov).